의학박사 학위논문

Role of integrin β4 expression in glioblastoma invasion and proliferation

교모세포종의 침윤과 증식에서 integrin $\beta 4$ 발현의 역할

2018 년 2 월

서울대학교 대학원

의학과 중개의학전공

이 규 상

ABSTRACT

Role of integrin β4 expression in glioblastoma invasion and proliferation

Kyu Sang Lee
Department of Medicine, Translational Medicine Major
The Graduate School
Seoul National University

Background: Glioblastoma (GBM) is the most malignant form of glioma and characterized by aggressive local invasiveness, making complete surgical resection of the cancer nearly impossible. To identify mechanisms of GBM invasion, we isolated highly invasive cells from the U87MG cell line via adhesion to a laminin-2 substrate and comparatively analyzed characteristics of U87MG and U373MG cells. Furthermore, we focused and analyzed the function, clinicopathologic features and prognosis of integrin β4 expression in GBM.

Methods: We selected the first 10% of invading cells (U87-Inv) from the U87MG GBM cell line using laminin-2-coated Transwell filters. To characterize the highly invasive cells, we performed a wound-healing assay and proliferation assay. Also,

we evaluated the expression of invasion-related factors, including gelatin zymography for matrix metalloproteinase-2 (MMP-2), immunofluorescence for fascin and actin, real-time quantitative polymerase chain reaction (RT-qPCR) for integrin subunits and western blot for fascin, Akt, and Erk. To focus and evaluate the function of integrin β4, we used the method of pRK5 β4 plasmid DNA transfection for U87MG and knockout with integrin β4 shRNA for U373MG. Moreover, integrin β4 expression was determined using immunohistochemistry (IHC) in a retrospective cohort of 89 consecutive patients with GBM. Cytoplasmic staining of moderate to strong intensity in neoplastic cells was considered positive staining. In addition, epidermal growth factor receptor (EGFR), p53, and isocitrate dehydrogenase 1 (IDH-1) expressions and Ki-67 were investigated by IHC.

Results: The migration rate of U87-Inv cells increased approximately 20% compared with that of the relatively less invasive cells (U87-Non). U87-Inv cells demonstrated faster wound healing, but lower proliferative activity. U87-Inv cells also showed extensive lamellipodia with the expression of fascin and actin, an increase in the activity of MMP-2, but a decrease in the expression of Erk. The expression of integrins α1 and α7 in U87-Inv cells increased approximately 1.5-fold, whereas that of integrins α6 and β4 was reduced by approximately 0.4- and 0.6-fold, respectively. Interestingly, U373MG cells showed slower migration rate and more increased proliferation rate than that of the U87MG cells. Moreover, U373MG showed markedly increased integrin β4 expression compared with that of U87MG cells. The pRK5 β4 transfected U87MG cells showed slower migration rate and more increased proliferation rate than that of the control U87MG cells. The integrin β4 knockout U373MG cells showed faster migration rate and more

decreased proliferation rate than that of the control U373MG cells. Our findings suggest that expression of integrin β4 is positively correlated with proliferation and negatively with invasiveness in GBM cell line. In GBM patients, positive staining for integrin β4 was observed in 33 (37.1%). Integrin β4 expression was significantly correlated with Ki-67 expression and negatively with tumor multiplicity and relapse. Therefore, integrin β4 expression seems to play an important role in proliferation and non-invasiveness in GBM patients. However, Kaplan–Meier analysis indicated that integrin β4 expression was not correlated with overall survival in GBM patients.

Conclusion: Using a laminin-2 substrate, we successfully isolated a subpopulation of highly invasive GBM cells. The highly invasive GBM cells likely showed a decrease in proliferation because of Erk inactivation via integrins α6 and β4. Moreover, we focused on evaluation of role of integrin β4 in both GBM cell line and tissue. Notably, the clinicopathological feature and prognosis were investigated in integrin β4 expressed GBM patients. In conclusion, our findings suggest that expression of integrin β4 is negatively associated with invasiveness and positively with proliferation in GBM.

Keywords: Glioblastoma, integrin β4, invasiveness, proliferation, laminin-2

Student number: 2012-30558

CONTENTS

Abstract ..... **i**

Contents ..... **iv**

List of tables ..... **v**

List of figures ..... **vi**

Introduction **1**

Materials and Methods **4**

Results **16**

Discussion **42**

References **46**

Abstract in Korean **55**

LIST OF TABLES

Table 1 Clinicopathological characteristics of the 89 patients with glioblastoma (GBM) 31

Table 2 Correlation between integrin β4 expression and other molecular alterations in patients with glioblastoma (GBM) 35

Table 3 Correlation between integrin β4 expression and clinical behavior in patients with glioblastoma (GBM) 38

LIST OF FIGURES

Figure 1 Cell-laminin-2 adhesion. 5

Figure 2 Selection of the highly invasive U87MG cells 7

Figure 3 Comparison of motility and proliferation rate between U87-Non and U87-Inv cells..... 18

Figure 4 Expression of matrix metalloproteinase-2 (MMP-2) and fascin. 21

Figure 5 Expression of integrin subunits and downstream signaling molecules in U87-Non and U87-Inv cells. 23

Figure 6 Comparison of motility, proliferation rate and integrin β4 between U87MG and U373MG cells.. 25

Figure 7 Overexpression of integrin β4 in U87MG cells by pRK5 β4 plasmid DNA.. 28

Figure 8 Knockout of integrin β4 in U373MG cells by short hairpin (sh)RNA.. 29

Figure 9 Representative figures showing immunohistochemical staining for integrin β4, Ki-67, epidermal growth factor receptor (EGFR), p53 and isocitrate dehydrogenase 1 (IDH-1) antibodies in glioblastoma samples... 33

Figure 10 Correlation between integrin β4 expression and Ki-67 index by Mann-Whitney analysis.. 36

Figure 11 Comparison of integrin β4 expression between central and peripheral lesions of glioblastoma (GBM) 39

Figure 12 Kaplan–Meier survival curves illustrating the prognostic effects of integrin β4 expression in glioblastoma.. 40

INTRODUCTION

Glioblastoma (GBM) is the most malignant form of glioma. Most patients demonstrate poor survival rates because of the aggressive and invasive character of GBM (1). This aggressive invasiveness may be key to understanding the failure of treating GBM. A single GBM cell can detach from a primary tumor and disseminate to myelinated fiber tracts of the white matter, which contains extracellular matrix (ECM) proteins. The ECM proteins of the brain include mainly laminin, type IV collagen, tenascin, fibronectin, and hyaluronic acid (2, 3). Laminins are a large family of multidomain αβγ heterotrimeric glycoproteins found in basement membranes (4). Laminin-2, which is composed of the α2, β1, and γ1 heterotrimeric chain, is first found in the basement membrane of the placenta, striated muscle, and Schwann cells (5, 6). The α2 subunit of laminin-2 is expressed in skeletal muscle and other tissues, including the peripheral (PNS) and central nervous system (CNS) (7). In the peripheral nervous system, a mutation in the *LAMA2* gene, which causes a deficiency in the laminin-2 α2 chain, can cause congenital muscular dystrophy (CMD) (8). Furthermore, laminin-2 plays an important role in myelinogenesis and promotes axonal growth in the CNS (9, 10). Nevertheless, an association between laminin-2 and tumors of the CNS has not been established.

Similar to other cancers, GBM is heterogeneous at its cellular and molecular levels (11, 12). The heterogeneity of GBM includes markedly different karyotypes in fresh tissue specimens and cell lines (13, 14), highlighting the necessity to isolate the highly invasive GBM cells in order to study their invasive capacity. A

previous study, using an invasive subpopulation of U87MG human GBM cells, evaluated their ability to invade through a collagen substrate and found that the upregulation of matrix metalloproteinase-2 (MMP-2) increases the invasive capacity of GBM cells (15). Therefore, in our study, we selected the highly invasive GBM cells on the basis of their adhesion to a laminin-2 substrate.

Laminin-2 performs numerous biological functions in cell adhesion, migration, proliferation, and differentiation (16). Laminin-2 mediates these functions through cell-surface receptors, particularly the integrin family of receptors (17, 18). Integrins are non-covalently linked heterodimeric transmembrane receptors for ECM molecules. Integrins are classified into several subfamilies on the basis of their ligand specificities. For example, integrins α3, α6, α7, and β4 mainly bind to laminin, whereas integrins α5, β3, β5, β6, and β8 mainly bind to the tripeptide Arg-Gly-Asp (RGD) receptor (19). Previous studies show that invasion in various cancers may be influenced by the integrin-mediated tumor cell-ECM interactions (20, 21). RGD-binding integrins α5β3 and α5β5 are over-expressed in glioma cells and tumor-associated vasculature (22). Cilengitide, a potent inhibitor of integrins α5β3 and α5β5, has been evaluated in clinical studies (23, 24). The laminin-binding integrins α3 and α6, have been shown to regulate the stem-like glioma cells (25, 26), and integrin β4 regulates GBM proliferation (27). However, the role of laminin-binding integrins in GBM remains to be determined.

The integrin-mediated adhesion of tumor cells influences diverse intracellular signaling pathways, including those mediated by phosphoinositide-3-kinase (PI3K)/Akt and mitogen-activated protein kinases (MAPK)/Erk (28, 29). Previous reports show that Erk can control proliferation and invasion in GBM (30, 31),

whereas Akt activation is correlated with invasiveness and stemness (32). However, a deeper understanding of these downstream signaling effectors in GBM is needed.

To migrate, malignant cells need to remodel their cytoskeleton to form the cellular protrusions known as filopodia. Motility requires complex rearrangement of multiple actin-binding proteins. One of these proteins, fascin, induces the bundling of actin for cell protrusion, adhesion, and migration (33, 34). Fascin is upregulated in various human cancers (35-37). The GBM cell line, with *FSCN1*-knockdown, shows attenuated invasiveness in a rat model (36). Therefore, we investigated whether overexpression of fascin is an indicator of high invasiveness.

In this study, we isolated highly invasive cells from the U87MG cell line via adhesion to a laminin-2 substrate and analyzed various biological features such as morphology, motility, rate of proliferation, and the expression of molecules associated with invasion, including MMP-2, fascin, integrins, Erk, and Akt. Moreover, we compared the expression of integrin β4 with invasiveness and proliferation in U87MG and U373 cells. Notably, the clinicopathological feature and prognosis was evaluated in integrin β4 expressed GBM patients.

MATERIALS AND METHODS

1. Cell line and culture

The human GBM U87MG and U373MG cells were grown in minimal essential medium (MEM, Welgene, Daegu, South Korea) supplemented with 10% fetal bovine serum (FBS) and antibiotics in a humidified 5% CO2 atmosphere at 37°C.

2. Cell-substrate adhesion assay

To investigate adhesion on laminin-2, 96-well plates were coated with various concentrations of human laminin-2 (laminin-2; Millipore, Temecula, CA, USA) in serum-free MEM for 1 h at 37°C (Figure 1). Wells were washed three times with phosphate-buffered saline (PBS) and blocked with 0.5 % bovine serum albumin (BSA; Sigma, St. Louis, MO, USA) solution for 30 min at 37°C. Cells were seeded at a density of 5 × 104/well in the laminin-2-coated plates, which were then placed on ice for 30 min to allow for the rapid sedimentation of the cells. After incubating for 2 h at 37°C, the plates were subjected to vigorous agitation (300 rpm for 5 min on a horizontal rotor), then the medium and the non-adherent cells were aspirated and washed with PBS. The attached cells were fixed with 3.7% paraformaldehyde/PBS (v/v) for 15 min and stained with crystal violet for 15 min. After the dye solution was aspirated, cells were washed with PBS, air-dried, and eluted with 10 % acetic acid on a shaker for 20 min. Absorption was measured at 540 nm using an ELISA plate reader (iMark; Bio-rad, Hercules, CA, USA).

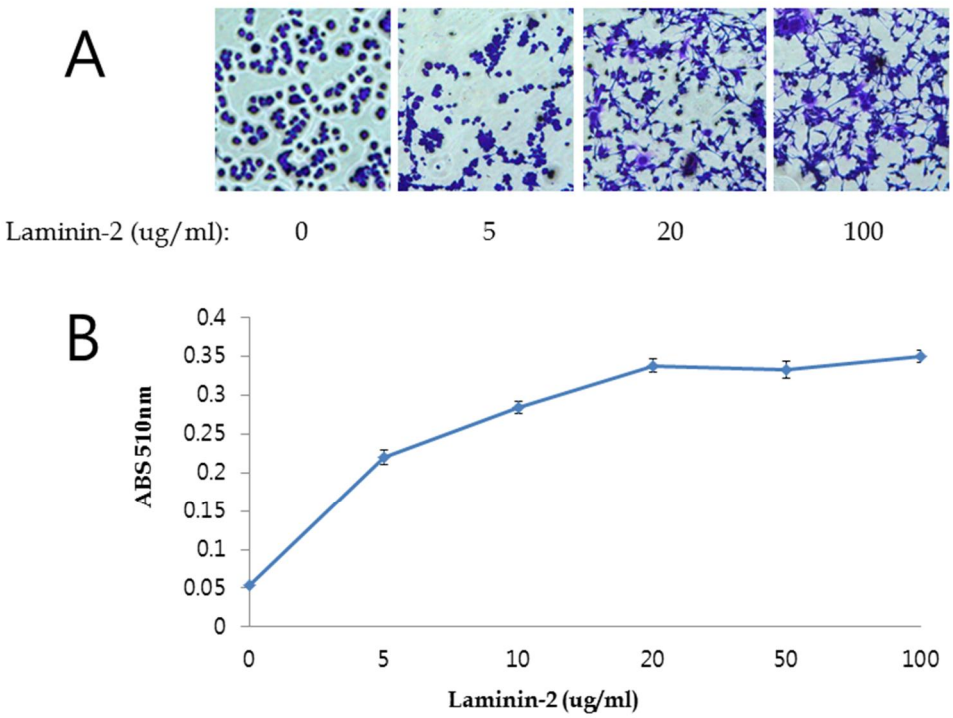

Figure 1. Cell-laminin-2 adhesion. A. Morphology of U87MG cells in laminin-2-coated wells coated with various concentrations of laminin-2. Morphology of U87MG cells is changed, showing longer neurite-like extensions in a dose-dependent manner. B. Each point represents the average optical absorbance, at 510 nm, in four independent experiments. Results are shown as mean ± SEM (n = 3). Statistical analysis was performed by the Mann-Whitney U test; asterisks indicate a statistically significant change ($P < 0.05$) in adhesion. The maximal effect of adhesion was achieved at a laminin-2 concentration ≥ 20 µg/mL.

3. Selection of highly invasive U87MG cells (U87-Inv)

U87-Inv cells were selected using a previously described method with modifications (Figure 2) (15). Transwell polycarbonate membrane inserts, with 8.0-μm pores (Corning Inc., NY, USA), were coated on the underside with 100 μg/mL of laminin-2. Cell suspensions were seeded onto the filters and allowed to migrate for approximately 3 h in a CO_2 incubator in the absence of serum. Cells that had migrated to the bottom of the inserts were detached and labeled with a cell dissociation solution (Trevigen, Gaithersburg, MD, USA) and the fluorescent dye calcein acetoxymethylester (Calcein AM, BD, Bedford, MA, USA) for 1 h in a CO_2 incubator. Calcein AM is internalized by the cells, and hydrolyzed by intracellular esterases, into the fluorescent anion calcein. The fluorescence of free calcein was used to quantify the number of cells, which had invaded out of the total seeded cells. After removing the inserts, the detached cells were transferred to a black plate, which was read at the excitation of 494 nm/emission 517 nm. Data are presented as a percentage of invading cells. The invading cells were visualized and photographed under a fluorescent microscope. To select for U87-Inv cells, the first 10% of the invading cells from U87MG were collected using the laminin-2-coated Transwell under serum-free conditions. The incubation time, required for approximately 10% of the cells to invade, was circa 3 h; the invading cells were harvested by brief, gentle trypsinization and cultured in new dishes. The selected cells were subsequently expanded and designated as U87-Inv. U87-Non (non-invading cells) on the upper surface of the filters were transferred to another dish and cultured separately.

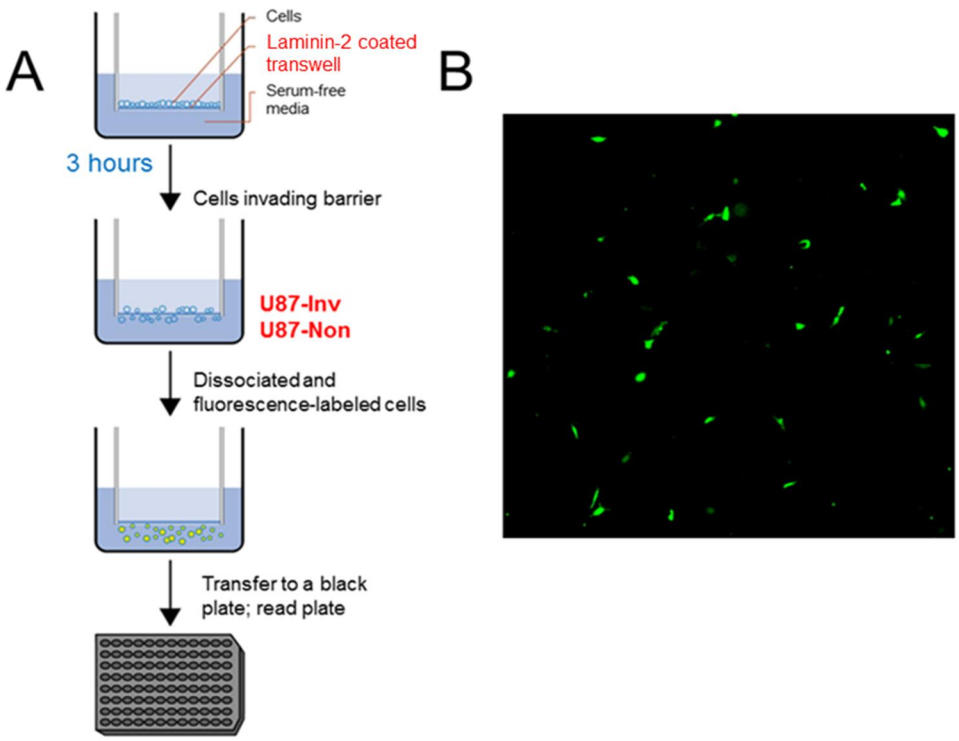

Figure 2. Selection of the highly invasive U87MG cells. A. Incubation time, required for roughly 10% of the cells to invade through the laminin-2-coated Transwell, was determined to be approximately 3 h. Cells, which had invaded to the bottom of the inserts, were designated as "U87-Inv", whereas non-invading cells on the upper surfaces of the filters were designated as "U87-Non;" U87-Non were collected and cultured separately. B. The invading cells were labeled with the calcein AM fluorescent dye and visualized under a fluorescent microscope.

4. Zymography

The production of MMP-2 was detected by gelatin zymography. Serum-free conditioned media were electrophoresed for 48 h on 8 % SDS-PAGE, containing 0.1% gelatin, under non-reducing conditions. Then, the gels were washed with 2.5% Triton X-100 for 30 min at room temperature (21°C), and incubated with activation buffer (50 mM Tris, 0.2 M NaCl, 5 mM CaCl2, pH 7.6) overnight at 37°C. The gels were then stained with Coomassie Brilliant Blue R-250 and destained with a 30% methanol/10% acetic acid solution. Gelatinolytic activity was visualized as a transparent band against a blue background.

5. Wound-healing assay

The ability to migrate was assessed by a wound-healing assay. After confluent monolayers were prepared, a yellow p200 pipet tip was used to make a straight scratch across each monolayer. The wounded areas were imaged immediately after the induction of the wound (0 h) and captured at 8 and 24 h post wound induction. At the indicated time points, the images of 10 different areas were acquired, then the gap distance was measured and compared with that of the initial scratch.

6. Invasion assay

96-well ImageLock microplates (Essen Bioscience, MI, USA) were pre-coated for 1 hour with Matrigel. Cells were grown to confluence on ImageLock plates for

24h in a standard CO2 incubator, and wounded precisely by the 96-pin Wound-Maker provided with the IncuCyte™ (Essen Bioscience). After washing thoroughly with PBS to remove the detached cells, the cells were placed in the IncuCyte™ (Essen Bioscience) with cell culture media. The wound images were automatically monitored and quantified with the IncuCyte live-cell imager (Essen Bioscience) from the incubator at 1 hour intervals. The kinetics of the relative wound density (RWD) was analyzed by IncuCyteTM (Essen Bioscience) software.

7. Cell proliferation assay

The Ez-Cytox cell viability assay kit (Daeil Service, Seoul, South Korea) was used to measure proliferation. The cells were seeded in a 96-well plate at a density of 5×10^3 cells/well and cultured for the indicated times (1, 2, or 3 days) in MEM containing 1% FBS. The reagent from the kit was then added to each well. After incubating for 2 h, the plate was measured at the absorbance wavelength of 450 nm using an ELISA plate reader.

8. Immunofluorescence (IF) double staining

First, the cells were cultured in chamber slides (Lab-Tek II chamber slide™ system, Nunc, Naperville, USA), then fixed with 4% paraformaldehyde for 20 min and permeabilized with 0.5% Triton X-100 for 5 min. Non-specific binding was blocked with 1% BSA for 1 h and the cells were incubated with an anti-fascin

monoclonal antibody (Fascin 1 [55K-2]:sc-21743, Santa Cruz Biotechnology Inc., TX, USA) overnight at 4°C. After washing, the cells were incubated with a goat anti-mouse IgG-FITC (goat anti-mouse IgG-FITC:sc-2010, Santa Cruz Biotechnology Inc.) secondary antibody for 1 h at room temperature (21°C). For double staining with F-actin, the cells were additionally incubated with Alexa Fluor568 phalloidin (Invitrogen, MA, USA), then mounted and visualized using a Zeiss microscope (Carl Zeiss, Jena, Germany). The fluorescent images were captured with an AxioCam camera (Carl Zeiss).

9. SYBR Green real-time quantitative PCR

Total RNA was isolated using the TRIzol (TRIzol Reagent, Invitrogen, CA, USA) method according to the manufacturer's protocol. Four micrograms of total RNA was reverse-transcribed using the PrimeScript^{TM} 1st strand cDNA synthesis kit (TaKaRa Biotechnology, Shiga, Japan). Transcripts were quantified by SYBR green PCR amplification (BIOLINE, London, UK). The primers were designed, and RT-qPCR performed, as described previously (38). Primers were targeted against integrin α1, α2, α3, α6, α7, β1, β4, or β-actin. β-actin was used as an internal control gene for calculation of a RT-PCR normalization factor. Data were analyzed by the comparative CT method as follows (39):

$2^{-\Delta\Delta Ct}$, $\Delta\Delta C_T$ = (C_T gene of interest - C_T internal control; sample A) - (C_T gene of interest - C_T internal control; sample B).

10. Western blotting

Total cell lysates were extracted in lysis buffer (50 mM Tris, pH 7.4, 150 mM NaCl, 1% Triton X-100, and 0.1% SDS) containing a protease inhibitor cocktail (Roche, IN, USA). Lysates were separated by SDS-PAGE and transferred to a nitrocellulose membrane (BioScience, Dassel, Germany). The membrane was blocked with 3% skim milk and incubated overnight at 4°C with the following primary antibodies: anti-phospho-Erk1/2(Thr202/Tyr204) (Cell Signaling Technology, MA, USA), anti-phospho-Akt (Cell Signaling Technology), anti-fascin monoclonal (Santa Cruz Biotechnology Inc.), or anti-β-actin (Santa Cruz Biotechnology Inc.). Subsequently, the membranes were incubated with horseradish peroxidase-conjugated secondary antibodies (anti-mouse and anti-rabbit IgGs; Santa Cruz Biotechnology Inc.) and developed with ECL detection reagents (Pierce, IL, USA).

11. Plasmid DNA transfection and knockout with short hairpin RNA

For transient transfection with integrin β4, U87MG cells (5× 105 cells/well) were plated on a six-well plate and transfected with 1μg pRK5 β4 plasmid DNA (Addgene, MA, USA) or control pRK5 vector by the WelFect-Si™ transfection reagent (Welgene), in according to the manufacturer's protocol. For the generating of integrin β4 knockout cell lines, integrin β4 short hairpin (sh)RNA and control shRNA plasmids (Santa Cruz Biotechnology Inc.) transfected into U373MG cells

using the WelFect-Si™ transfection reagent (Welgene) and stable cell clones were generated with puromycin (0.5 ug/ml) selection.

12. Patients and tumor samples

This study included 89 patients with GBM who underwent radical surgery or stereotactic biopsy at the Seoul National University Bundang Hospital between May 2003 and February 2013. In total, 31 patients underwent stereotactic biopsy or partial resection and 58 underwent gross total resection. Two neuropathologists (K.S.L. and G.C.) reviewed the histopathology and confirmed GBM diagnoses for all lesions. The lesions were re-classified as per the fifth edition of the World Health Organization (WHO) classification of central nervous system tumors (40). Oligodendroglial tumors were excluded by 1p19q fluorescence in situ hybridization (FISH) testing. Even though IDH gene mutations were not evaluated by sequencing, the IDH1 R132H mutation status was assessed by immunohistochemistry (IHC). Clinicopathological information was obtained from hospital medical reports.

The Institutional Review Board of the Seoul National University Bundang Hospital approved the use of medical record data and tissue samples for this study (reference: B-1612/374-304).

13. Tissue array method

Two tissue microarrays (TMA) were constructed with formalin-fixed paraffin-embedded (FFPE) donor GBM tissues. For each patient, two cores (each of 3 mm diameter) from representative regions of the GBM tissues were punched out (ensuring >30% cancer cells in each sample), and transferred to a TMA recipient block.

14. Immunohistochemistry

Immunostaining using integrin β4 (EPR17517, 1:250, abcam, San Francisco, CA, USA), epidermal growth factor receptor (EGFR; 1:150, Dako, Camarillo, CA, USA), p53 (1:1000, Dako, Glostrup, Denmark), Ki-67 (1:50, Dako, Carpinteria, CA, USA) and isocitrate dehydrogenase 1 (IDH-1; 1:100, DIANOVA, Hamburg, Germany) antibodies was performed on each two TMA slides using the Ventana Bench mark XT autostainer (Ventana) with the ultraView Universal DAB kit (Ventana) according to the manufacturer's standard recommendations. Normal glial tissues served as internal negative controls. The intensity of integrin β4 (cytoplasmic) and EGFR (membranous) staining was graded as 0 (no cell stained), 1 (weak intensity), 2 (moderate) and 3 (strong). For statistical analysis, scores of 0 and 1 were considered to indicate negativity and scores of 2 and 3 were considered to indicate positive staining. The percentage of cells with p53 nuclear staining was counted; overexpression was recorded when tumor nuclei showed >10% staining. Positive IDH-1 expression was considered when cytoplasmic staining was observed in neoplastic cells

15. O(6)-methylguanine-DNA methyltransferase (MGMT) promoter methylation assay

DNA was extracted from GBM tissues and treated with bisulfite using the EZ DNA methylation kit (Zymo Research, Freiburg, Germany) according to the manufacturer's protocol. Methylation-specific polymerase chain reaction (PCR) was performed as previously described (41). The predicted fragment size was 80 bp for methylated PCR and 92 bp for non-methylated PCR. The PCR products were visualized on 4% agarose gels.

16. Fluorescence in situ hybridization (FISH) for the assessment of 1p/19q deletion

The LSI 1p36/LSI 1q25 DNA probe and LSI 19q13/LSI 19p13 DNA probe (Vysis, IL, USA) were used for 1p/19q FISH, which was performed according to the manufacturer's protocol. Briefly, 4-um thick paraffin slides were deparaffinized, dehydrated and incubated in solution at 80°C for 30 min. The slides were immersed in protease solution at 37°C for 20 min, and tissues were incubated in 10% buffered formalin. Then, the slides were hybridized with Hybrite (ThermoBriteTM vysis). After drying in darkness, 10 ul of counterstain was applied to the target region on the slide and a cover slip was placed. The FISH results were interpreted according to guidelines defined by the European Society for Paediatric Oncology

(SIOP Europe) Neuroblastoma Pathology and Biology and Bone Marrow Group (42).

17. Statistical analysis

Data were expressed as means ± standard error of the mean (SEM). Different treatments were compared by the Mann-Whitney U test, as indicated in the figure legends. The Pearson correlation coefficient was used for analyzing comparison between Ki-67 index and integrin β4 expression. Chi-square tests or Fisher's exact tests were used for the comparison of categorical variables as appropriate. Kaplan–Meier analysis with a log-rank test was used to evaluate survival curves. For all analyses, $P < 0.05$ was considered to be statistically significant. All cell line experiments were performed at least three times. Statistical analyses were performed using the SPSS 21 software (IBM Analytics, USA).

RESULTS

1. Effect of laminin-2 on U87MG adhesion

We performed an adhesion assay, which removes weakly attached cells by mechanical agitation, to assess whether U87MG cells can adhere to laminin-2 (Figure 1). The cells were plated on surfaces coated with various concentrations of human laminin-2. In a dose-dependent manner, laminin-2 induced an increase in the adhesive capacity of U87MG cells and led to a change in the morphology of the cells, which developed longer neurite-like extensions. Maximal adhesion was achieved at a 20 μg/mL, or greater, concentration of laminin-2. Laminin-2 was the most effective substrate for U87MG cell adhesion. Micrographs were acquired 2 h after incubating the cells on laminin-2-coated plates.

2. U87-Inv cells showed increased motility

A migration assay was performed using a non-coated membrane. Cells were plated under serum-free conditions, and medium, containing 10% FBS as the chemoattractant, was added to the lower chamber. After 4 h of incubation, cells that had migrated to the bottom side of the inserts were quantified using calcein AM fluorescent dye. The migration rate of U87-Inv cells was approximately 20% higher than that of U87-Non cells (Figure 3A). A wound-healing assay was performed to confirm this difference in migration capacity. Cells were seeded as a high-density monolayer, and wound healing was observed at 8, 16, and 24 h after inducing a scratch with a p200 pipette tip (Figure 3B). After 8 h, U87-Inv cells

rapidly migrated into the wounded area, and the wounds were nearly healed after 24 h. Conversely, the parental (Par) and U87-Non cells showed slower migration rate than that of the U87-Inv cells; consequently, closure of the wound was also slower (Figure 3C). Interestingly, the proliferation rate of U87-Inv cells was significantly reduced compared with that of U87-Non cells (Figure 3D).

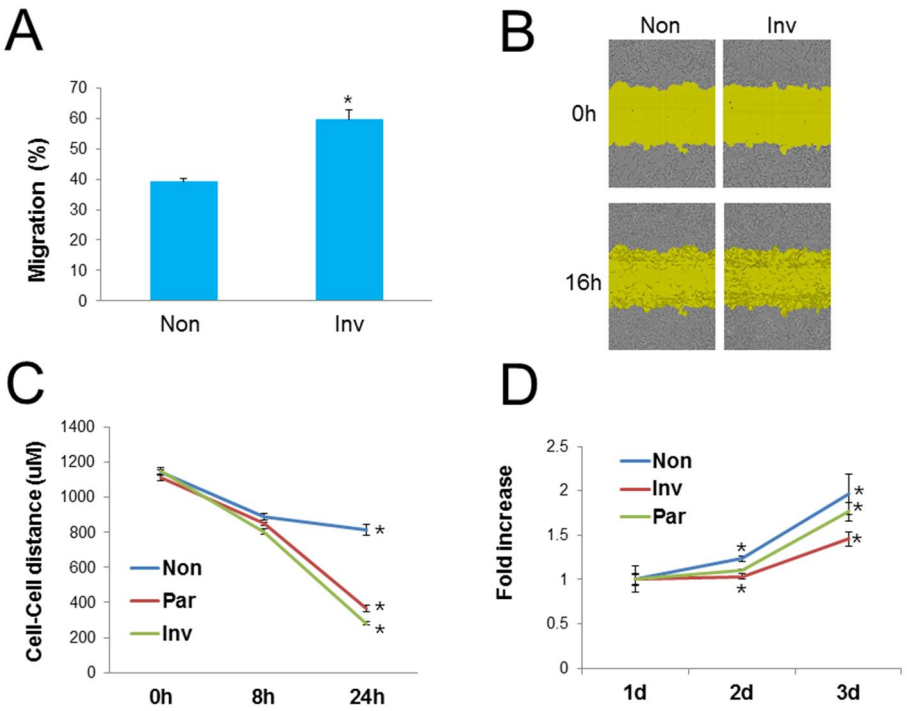

Figure 3. Comparison of motility and proliferation rate between U87-Non and U87-Inv cells. A. A migration assay was first performed with the non-coated membrane. After 4 h of incubation, cells that had migrated to the bottom side of the inserts were quantified using the calcein AM fluorescent dye. U87-Inv cells show a 1.5-fold increased motility compared with that of the U87-Non cells. Results are shown as mean ± SEM (n = 3). Statistical analysis was performed by the Mann-Whitney U test; asterisks indicate statistically significant change ($P < 0.05$). B. Wound-healing was monitored at 8, 16, and 24 h after scratching the surface of the plate with a pipette tip. C. The area of the gap between the migrating edges of the cells was used to quantify the assay by measuring 10 different distances at random. The cells to recover more rapidly (in order) were the U87-Inv cells, followed by the U87MG parental cell line (U87-Par), and the U87-Non cells. Results are shown

as mean ± SEM (n = 10). Statistical analysis was performed by the Mann-Whitney U test; asterisks indicate statistical significance ($P < 0.05$). D. Cell proliferation was determined using Ez-Cytox. U87-Inv cells show lower proliferation compared with that of U87-Non cells. Results are shown as mean ± SEM (n = 3). Statistical analysis was performed by the Mann-Whitney U test; asterisks indicate statistically significant changes ($P < 0.05$).

3. U87-Inv cells showed an increased level of MMP-2

The expression of MMP-2, an important factor in GBM invasion, was investigated by zymography (43, 44). Our result showed that the expression of MMP-2 increased in U87-Inv cells compared with that in U87-Non cells (Figure 4A).

4. U87-Inv cells displayed cytoskeletal features of high motility

We assessed the localization of fascin expression because fascin is a major regulator of cell motility and cytoskeletal alterations. Western blotting indicated that U87-Inv cells had an increased expression of fascin (Figure 4B). Additionally, U87-Inv cells showed extensive lamellipodia. Fluorescence double-staining revealed that fascin was expressed in the part of filamentous actin (F-actin)-rich protrusive structures in U87-Inv cells (Figure 4C).

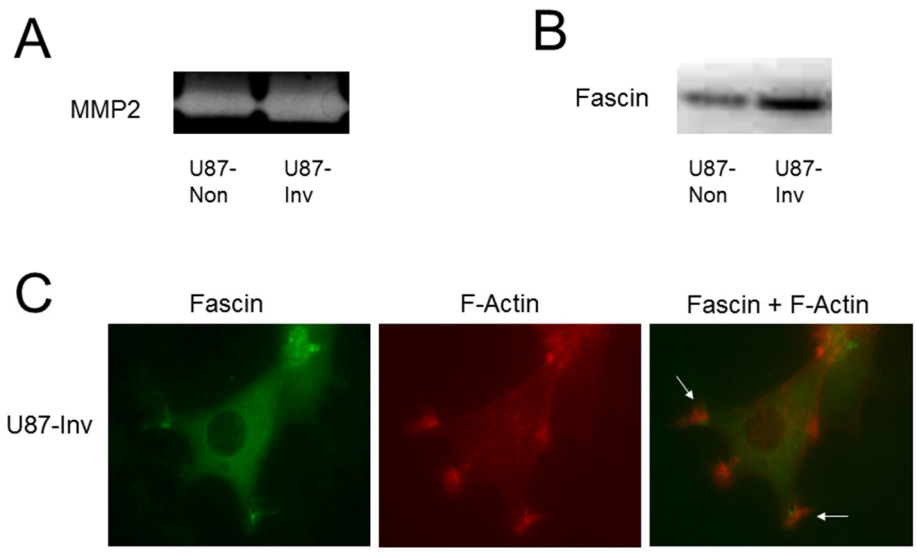

Figure 4. Expression of matrix metalloproteinase-2 (MMP-2) and fascin. A. Expression of MMP-2 was analyzed by zymography. U87-Inv cells show an increased expression level of MMP-2 compared with that of U87-Non cells. B. U87-Inv cells show an increase in fascin expression as assessed by western blotting. C. Expression and localization of fascin was detected by immunofluorescence. Arrows show co-localization of fascin and F-actin, demonstrating bundles of filopodia.

5. Expression of integrin receptors in U87-Non and U87-Inv cells

We analyzed whether the expression levels of laminin-2-binding integrins differed between U87-Non and U87-Inv cells (Figure 5A). The expression of mRNAs encoding integrins α1, α2, α3, α6, α7, β1, and β4 was examined by RT-qPCR (6). The expression of integrins α1 and α7 was increased by approximately 1.5-fold in U87-Inv cells. The expression of integrins α6 and β4 was reduced by approximately 0.4- and 0.6-fold, respectively, in U87-Inv cells compared with that in U87-Non cells. There was no significant difference in the expression of integrins α2, α3, and β1 between U87-Inv and U87-Non cells.

6. Erk and Akt expression in U87-Non and U87-Inv cells

We investigated the expression of integrin-related molecules Erk and Akt, which are involved in proliferation and invasion (Figure 5B). The expression of phospho-Erk was significantly upregulated in U87-Non cells compared with that in U87-Inv cells. There was no difference in the expression of phospho-Akt between U87-Non and U87-Inv cells.

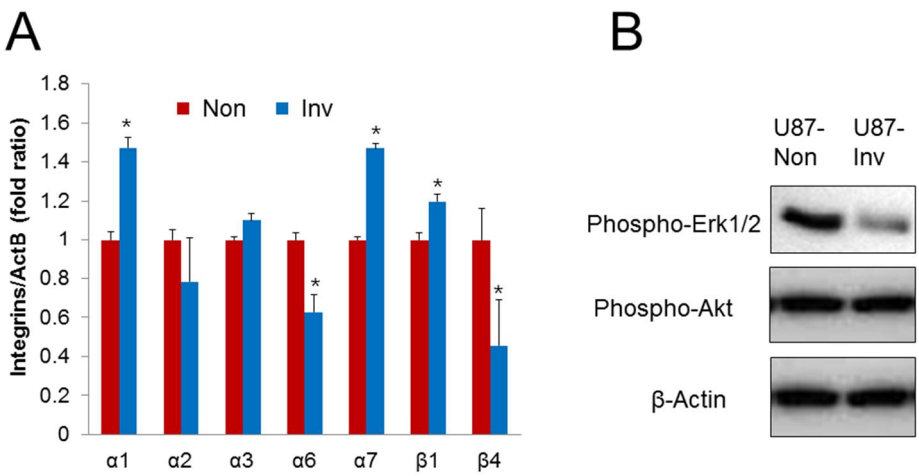

Figure 5. Expression of integrin subunits and downstream signaling molecules in U87-Non and U87-Inv cells. A. Expression of mRNAs encoding integrins α1, α2, α3, α6, α7, β1, and β4, which are known receptors for laminin-2, was investigated by real-time quantitative PCR (RT-qPCR). U87-Inv cells show an increased expression level of integrins α1 and α7 compared with that in U87-Non cells, whereas the expression of integrins α6 and β4 is reduced in U87-Inv cells. Results are shown as mean ± SEM (n = 3). Statistical analysis was performed by the Mann-Whitney U test; asterisks indicate statistically significant changes (P < 0.05). B. Cellular proteins were resolved on 6-10% SDS-polyacrylamide gels. Membranes were probed with anti-phospho-Erk1/2 or phospho-Akt primary antibodies. β-actin was used as loading control. U87-Inv cells show a decrease in the levels of phosphorylated Erk1/2.

7. Comparison analysis between the U87MG and U373MG cells

We attempted comparative analysis to determine the difference between U87MG and U373MG cells. U373MG cells showed slower migration rate than that of the U87MG cells (Figure 6A); consequently, closure of the wound was also slower (Figure 6B). The proliferation rate of U87MG cells was significantly reduced compared with that of U373MG cells (Figure 6C). Interestingly, U373MG showed markedly increased integrin β4 expression compared with that of U87MG cells in RT-PCR and western blot (Figure 6D and 6E). However, there is no significant difference in the integrin α6 expression.

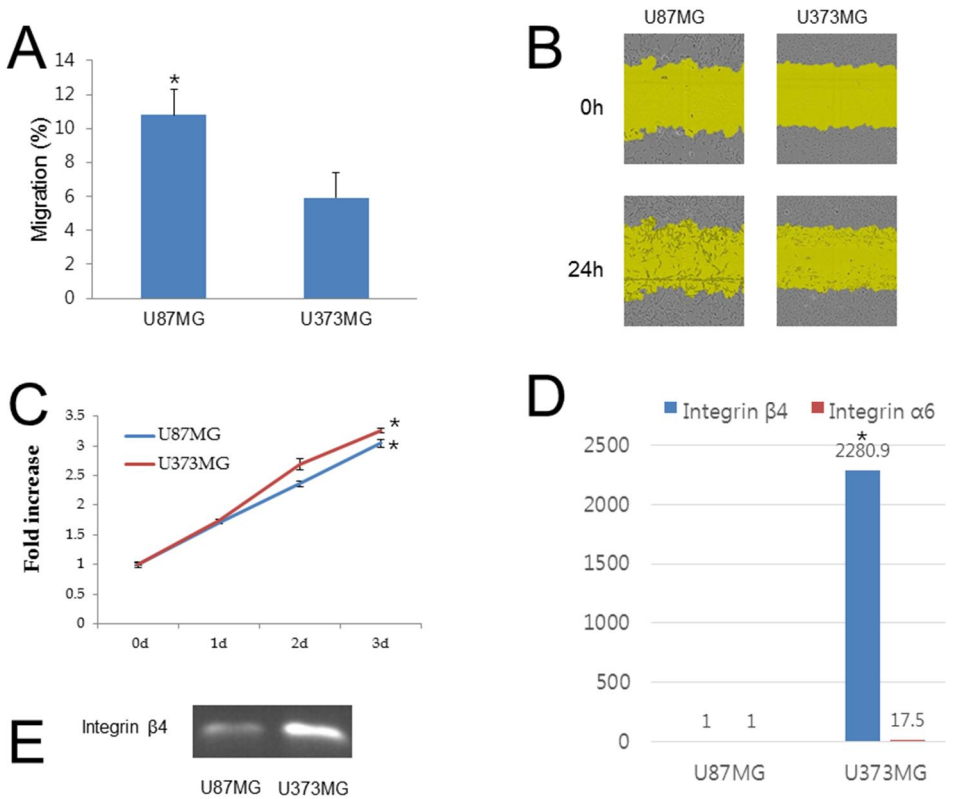

Figure 6. Comparison of motility, proliferation rate and integrin β4 between U87MG and U373MG cells. A. U87MG cells show a 1.8-fold increased motility compared with that of the U373MG cells. Results are shown as mean ± SEM (n = 3). Statistical analysis was performed by the Mann-Whitney U test; asterisks indicate statistically significant change ($P < 0.05$). B. Wound-healing was monitored at 8, 16, and 24 h after scratching the surface of the plate with a pipette tip. C. Cell proliferation was determined using Ez-Cytox. U87MG cells show lower proliferation compared with that of U373MG cells. Results are shown as mean ± SEM (n = 3). Statistical analysis was performed by the Mann-Whitney U test; asterisks indicate statistically significant changes ($P < 0.05$). D. U373MG cells show markedly increased expression level of integrin β4 compared with that in U87MG cells, whereas there is no significant difference in the integrin α6

expression by real-time quantitative PCR (RT-qPCR). Results are shown as mean ± SEM (n = 3). Statistical analysis was performed by the Mann-Whitney U test; asterisks indicate statistically significant changes ($P < 0.05$). E. U373MG cells show an increase in the levels of integrin β4 by western blotting.

8. Transfection and knockout of integrin β4 in U87MG and U373MG cells

We used transfection and knockout methods to determine the role of integrin β4 in GBM cell line. The pRK5 β4 plasmid DNA was successfully inserted into the U87MG cells and the transfected cells exhibit overexpression of the integrin β4 (Figure 7A). The pRK5 β4 transfected U87MG cells showed slower migration rate than that of the control U87MG cells (Figure 7B and 7C). The proliferation rate of pRK5 β4 transfected U87MG cells was significantly increased compared with that of control U87MG cells (Figure 7D).

The integrin β4 shRNA was successfully inserted into the U373MG cells for knockout integrin β4 gene (Figure 8A). The integrin β4 knockout U373MG cells showed faster migration rate than that of the control U373MG cells (Figure 8B and 8C). The proliferation rate of integrin β4 knockout U373MG cells was significantly reduced compared with that of control U373MG cells (Figure 8D). Our findings suggest that expression of integrin β4 is correlated with proliferation and negatively with invasiveness in GBM cell lines.

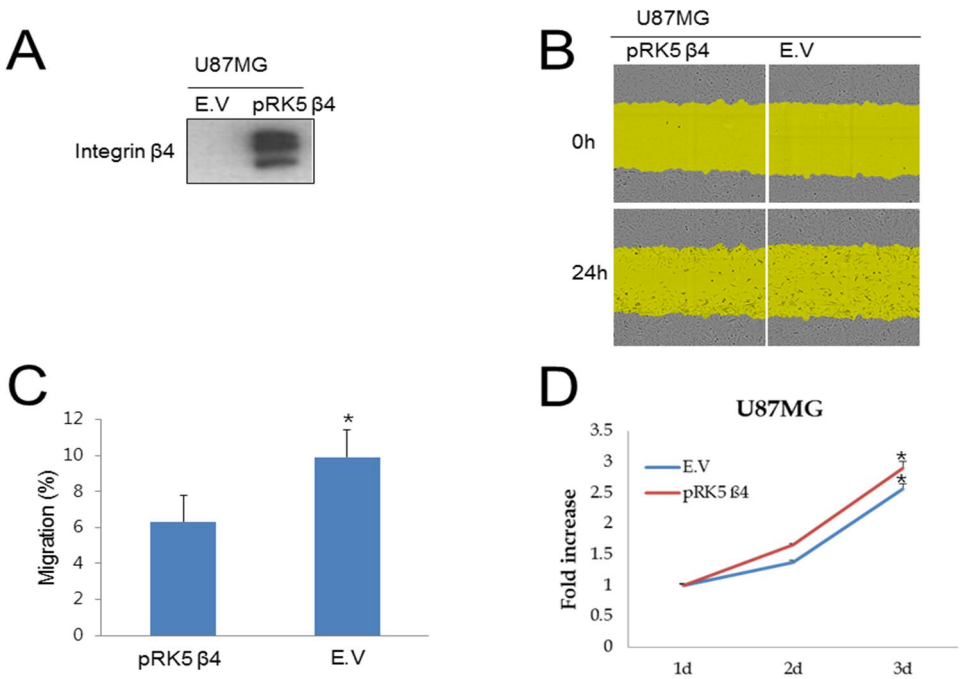

Figure 7. Overexpression of integrin β4 in U87MG cells by pRK5 β4 plasmid DNA. A. The U87MG cells is successfully transfected with pRK5 β4 plasmid DNA and shows overexpression of the integrin β4. B. Wound-healing was monitored at 8, 16, and 24 h after scratching the surface of the plate with a pipette tip. C. The pRK5 β4 transfected U87MG cells show a 0.6-fold decreased motility compared with that of control U87MG cells. Results are shown as mean ± SEM (n = 3). Statistical analysis was performed by the Mann-Whitney U test; asterisks indicate statistically significant change ($P < 0.05$). D. Cell proliferation was determined using Ez-Cytox. The pRK5 β4 transfected U87MG cells show higher proliferation rate compared with that of control U87MG cells. Results are shown as mean ± SEM (n = 3). Statistical analysis was performed by the Mann-Whitney U test; asterisks indicate statistically significant changes ($P < 0.05$).

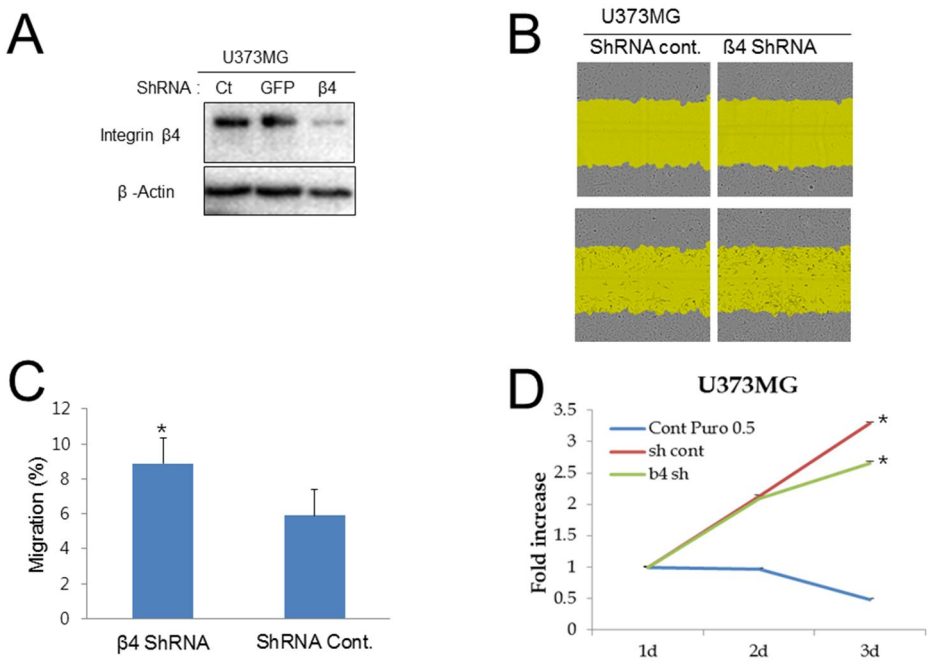

Figure 8. **Knockout of integrin β4 in U373MG cells by short hairpin (sh)RNA.** A. The integrin β4 shRNA successfully knockout the integrin β4 of U373MG cells. B. Wound-healing was monitored at 8, 16, and 24 h after scratching the surface of the plate with a pipette tip. C. Integrin β4 knockout U373MG cells show a 1.5-fold increased motility compared with that of control U373MG cells. Results are shown as mean ± SEM (n = 3). Statistical analysis was performed by the Mann-Whitney U test; asterisks indicate statistically significant change (P < 0.05). D. Cell proliferation was determined using Ez-Cytox. The Integrin β4 knockout U373MG cells show lower proliferation compared with that of control U373MG cells. Results are shown as mean ± SEM (n = 3). Statistical analysis was performed by the Mann-Whitney U test; asterisks indicate statistically significant changes (P < 0.05).

9. Clinicopathological characteristics of GBM patients

Table 1 demonstrates the clinicopathological characteristics of the patients included in this study. The average age was 58.3 (20–81) years. Approximately half the GBM lesions originated from the temporal lobe (48.3%). At the time of diagnosis, three GBM lesions had already involved multiple sites. One patient exhibited primary cerebellar GBM. Secondary GBM, which originates from a low-grade glioma, was observed in eight (9.0%) patients. The incidence rate of secondary GBM was similar to that in previous studies (45, 46). In total, 58 (65.2%) patients underwent gross total resection. The post-operative therapy including temozolomide (TMZ) and radiotherapy was performed in 74 (83.1%) and 80 (89.9%) patients, respectively. All patients who received TMZ also received radiotherapy. Recurrence after surgical treatment was observed in 37 (38.3%) patients. Forty-eight (53.9%) patients received conventional therapy (gross total resection plus TMZ and radiotherapy). Recurrence after surgical treatment was observed in 37 (41.6%) patients.

Table 1. Clinicopathological characteristics of the 89 patients with glioblastoma (GBM)

		Entire Population (No = 89)	
		Number	Percent (%)
Age	Mean (Range)	59.3 (20-84)	
Tumor location	Frontal lobe	22	24.7%
	Temporal lobe	43	48.3%
	Parietal lobe	13	14.6%
	Brain stem	7	7.9%
	Mutiple lobes	3	3.4%
	Cerebellun	1	1.1%
Hemispheres	Right	46	51.7%
	Left	34	38.2%
	Not evaluable	9	10.1%
Type	Primary GBM	81	91.9%
	Secondary GBM	8	9.0%
Extent of procedure	Biopsy	8	9.0%
	Partial resection	23	25.8%
	Grossly total resection	58	65.2%
Radiotheraphy	No	9	10.1%
	Yes	80	89.9%
Temozolomide	No	15	16.9%
	Yes	74	83.1%
Recurrence after treatment	No	52	58.4%
	Yes	37	41.6%

Abbreviations: GBM, glioblastoma; No, number

10. Frequency of integrin β4 expression and other molecular alterations in GBM patients

We immunohistochemically investigated integrin β4, EGFR, p53, ki-67 and IDH-1 expressions in GBM tissues (Figure 9). All 89 GBM tissues were stained for integrin β4 and IDH-1. Integrin β4 expression was primarily represented by a cytoplasmic staining pattern in tumor cells. Negative (scores 0 and 1) and positive (scores 2 and 3) staining for integrin β4 were observed in 56 (62.9%) and 33 (37.1%) samples, respectively. Expression of IDH-1, a specific marker for the detection of IDH-1 (R132H) mutations (45), was observed in nine (10.1%) samples, in agreement with previously published data (46). All secondary GBM samples expressed IDH-1. In total, 86 GBM samples were available for Ki-67, EGFR and p53 staining. EGFR positivity (scores 2 and 3) and p53 overexpression (>10%) were observed in 62 (72.1%) and 43 (39.5%) samples, respectively. High Ki-67 index (>20%) were present in 25 (29.1%) samples. MGMT methylation was observed in 18 (31.6%) of 57 GBM samples. Co-deletion of 1p/19q was not observed in all GBM samples.

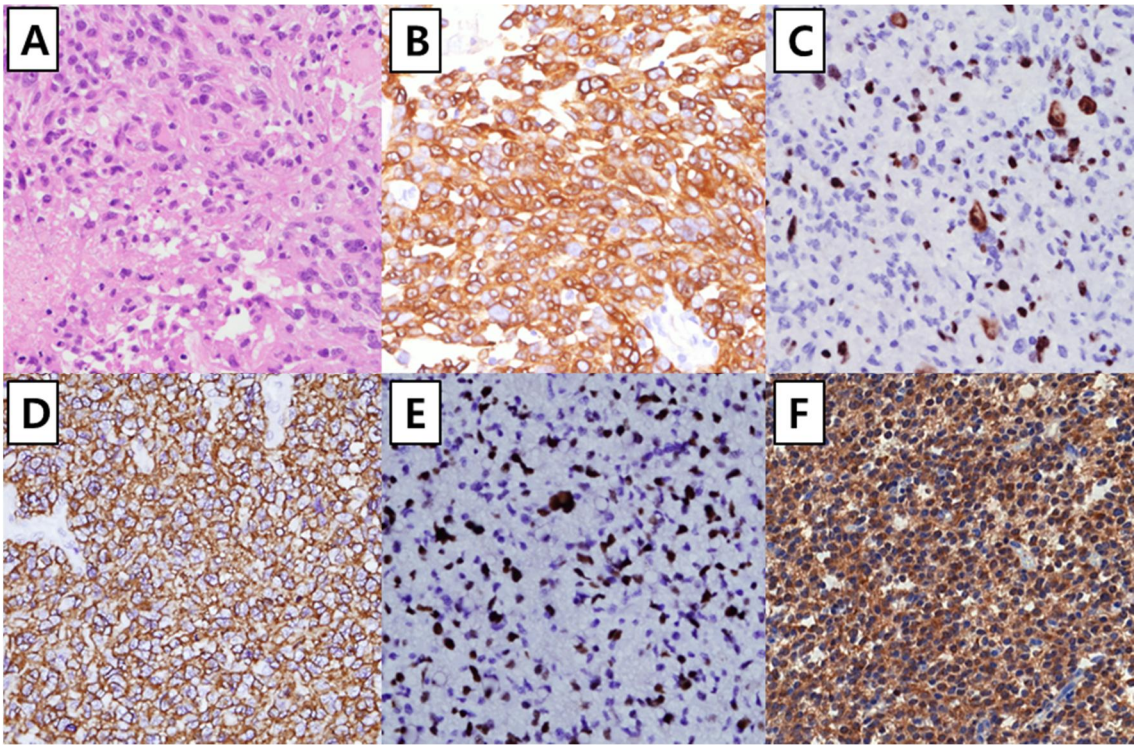

Figure 9. Representative figures showing immunohistochemical staining for integrin β4, Ki-67, epidermal growth factor receptor (EGFR), p53 and isocitrate dehydrogenase 1 (IDH-1) antibodies in glioblastoma samples. A. Hematoxylin and eosin stain (×400). B. Integrin β4 expression (score 3) (×400). C. Ki-67 expression (positive in 25% tumor cells) (×400). D. EGFR expression (score 3) (×400). E. p53 expression (positive in 50% tumor cells) (×400). F. IDH-1 expression (×400).

11. Correlation between integrin β4 expression and other molecular alterations in GBM patients

Table 2 presents the correlations between integrin β4 expression and other molecular alterations in GBM. Integrin β4 expression was significantly associated with high Ki-67 index (>20%) ($P = 0.001$). Also, integrin β4 expression was significantly correlated with Ki-67 expression in Mann-Whitney U test (Figure 10: $P < 0.001$). Since Ki-67 is key marker of tumor proliferation, integrin β4 expression seems to play an important role in GBM proliferation.

Table 2. Correlation between integrin β4 expression and other molecular alterations in patients with glioblastoma (GBM)

		Total No.	Integrin β4				*p*-value
			Negative		Positive		
IDH-1	Negative	80	50	89.3%	30	90.9%	0.806
	Positive	9	6	10.7%	3	9.1%	
EGFR	Negative	24	12	22.2%	12	37.5%	0.127
	Positive	62	42	77.8%	20	62.5%	
p53	Negative	52	36	66.7%	16	50.0%	0.127
	Positive	34	18	33.3%	16	50.0%	
Ki-67	< 20%	61	45	83.3%	16	50.0%	**0.001**
	≥ 20%	25	9	16.7%	16	50.0%	
MGMT	Non-methylated	39	26	70.3%	13	65.0%	0.683
	Methylated	18	11	29.7%	7	35.0%	

Abbreviations: GBM, glioblastoma; No, number; EGFR, epidermal growth factor receptor; IDH-1, isocitrate dehydrogenase 1; MGMT, O(6)-methylguanine-DNA methyltransferase

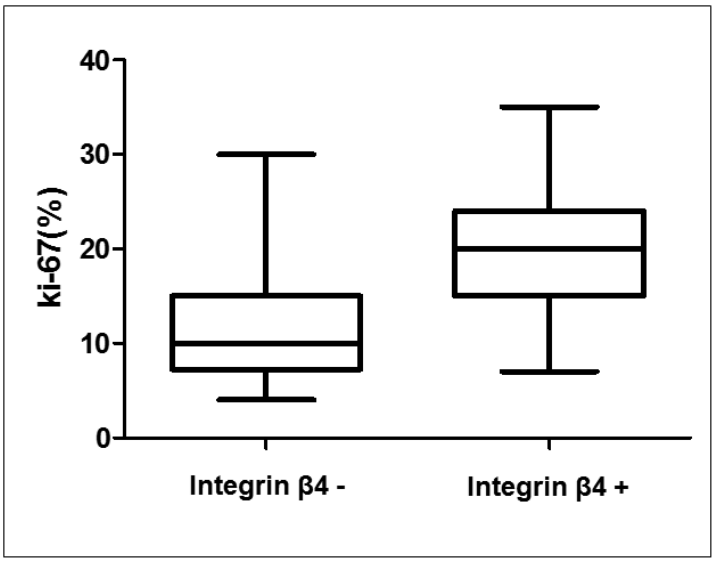

Figure 10. Correlation between integrin β4 expression and Ki-67 index by Mann-Whitney analysis.

12. Clinical behavior and prognostic impact of integrin β4 expression in GBM patients

Table 3 indicated that integrin β4 expressed GBM patients tend not to have tumor multiplicity and relapse. The tumor multiplicity and relapse are strongly associated with invasiveness of tumor. Therefore, we could suggest that integrin β4 expression is negatively correlated with invasiveness in GBM tissue, in consistent with our previous finding of cell line experiments.

For analysis the locational heterogeneity of integrin β4 expression, we investigated integrin β4 positive (score 3) GBM cases from the central and peripheral lesion (Figure 11). All of score 3 positivity cases (9 cases) were evaluated integrin β4 IHC in whole section of represent slide. Peripheral lesion of tumor was thought to be more invasive and integrin β4 expression was expected to be low. However peripheral lesions showed the same grade of integrin β4 expression as the central lesion. All cases had no locational heterogeneity.

Survival analysis was successfully conducted for all 89 patients (Figure 12). The mean follow-up duration was 22 months (range, 1–134 months), and 58 (65.2%) patients died during this period. Unfortunately, Kaplan–Meier analysis indicated that integrin β4 expression was not correlated with overall survival in all 89 patients ($P > 0.05$). EGFR expression, p53 overexpression and high Ki-67 index were not associated with survival ($P > 0.05$), whereas IDH-1 expression and MGMT methylation were significantly associated with improved survival ($P < 0.05$), in agreement with the findings of a previous studies (46, 47).

Table 3. Correlation between integrin β4 expression and clinical behavior in patients with glioblastoma (GBM)

		Total No. of cases	Integrin β4				*p*-value
			Negative		Positive		
Multiplicity	No	71	40	71.4%	31	93.9%	**0.011**
	Yes	18	16	28.6%	2	6.1%	
Recurrence after treatment	No	52	28	50.0%	24	72.7%	**0.036**
	Yes	37	28	50.0%	9	27.3%	

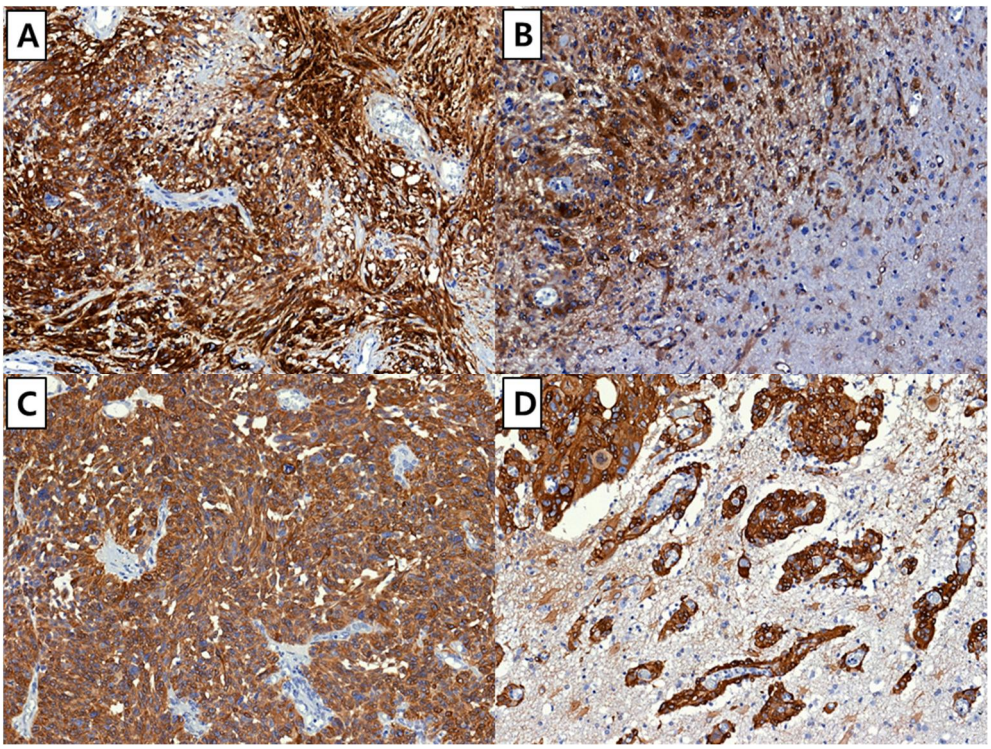

Figure 11. Comparison of integrin β4 expression between central and peripheral lesions of glioblastoma (GBM). A. Integrin β4 expression in center of tumor in case 1. B. Integrin β4 expression in periphery of tumor in case 1. C. Integrin β4 expression in center of tumor in case 2. D. Integrin β4 expression in periphery of tumor in case 2.

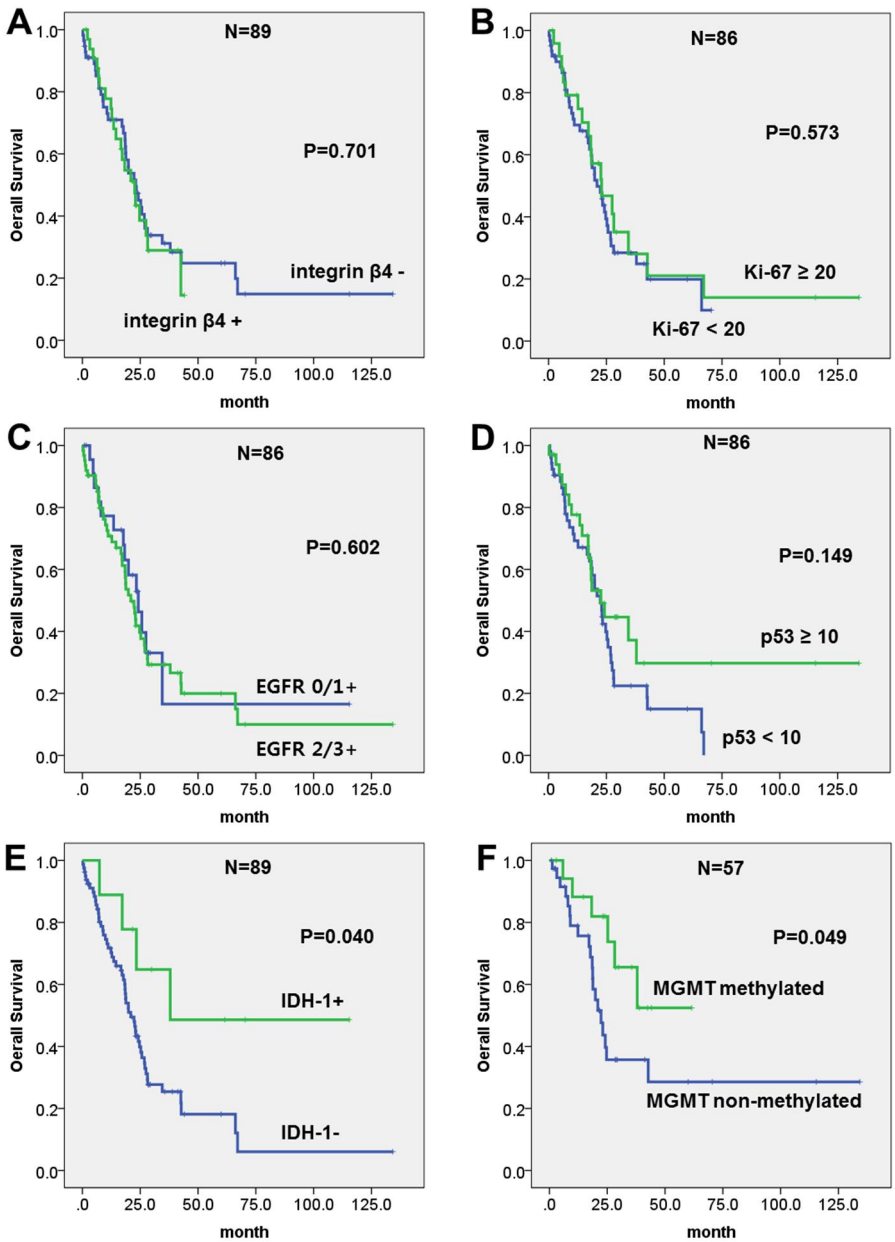

Figure 12. Kaplan–Meier survival curves illustrating the prognostic effects of integrin β4 expression in glioblastoma (GBM). A. Integrin β4 expression. B. Ki-67 expression. C. Epidermal growth factor receptor (EGFR) expression. D. p53

expression. E. Isocitrate dehydrogenase 1 (IDH-1) expression. F. MGMT methylation.

DISCUSSION

GBM extensively invades into the surrounding normal brain tissue, rendering complete surgical resection nearly impossible and resulting in a poor prognosis. We examined the highly invasive GBM cells for their heterogeneity at the cellular level (11, 12). A highly invasive subpopulation of GBM cells was selected according to previously described methods (15). Unlike previous studies, we used the laminin-2 substrate to examine adhesion because the ECM of the CNS is composed mainly of laminin-2 rather than collagen (48, 49). To investigate whether the selected cells were more invasive, we performed a migration assay to examine the motility of the cells, zymography to examine the expression of MMP-2, and immunofluorescence to assess the expression of fascin. Our results indicated that we had successfully selected a subpopulation of highly invasive cells.

We compared the expression of integrin receptors between U87-Non and U87-Inv cells (Figure 5A). The U87-Inv cells showed an increase in the expression of integrins α1 and α7. Integrin α1, a collagen receptor that can activate the Ras/Shc/mitogen-activated protein kinase pathway (19, 50), is also reported to drive the progression of non-small cell lung and colorectal cancers (51, 52). Integrin α7 is a laminin receptor that serves as a link between the extracellular matrix and the actin cytoskeleton (53). Hence, integrin α7 may suppress tumor growth and retard metastasis in several malignant tumors (54). The U87-Inv cells, overexpressing integrins α1 and α7, showed an increased ability to migrate but a decreased rate of proliferation. However, the mechanism of integrin α1 and α7 in GBM remains unclear and requires further investigation.

In contrast with the expression of integrin α1 and α7, our results indicate that U87-Inv cells showed a decrease in the expression of integrin α6 and β4. Integrin β4 binds distinctly only to α6 subunits (19). The expression of the laminin receptor of integrin α6β4 is correlated with tumor survival and angiogenesis in various malignancies (55-58). A previous study reported that integrin α6 enhances the proliferation of U87MG cells (59). GBM stem cells overexpress integrin α6 and their interaction with laminin on endothelial cells directly regulates tumorigenicity (26, 60). Other studies suggest that integrin α6β4 signaling promotes tumorigenesis and angiogenesis by enhancing the nuclear translocation of Erk (58), and that integrin β4 is involved in the regulation of GBM proliferation (27). Taken together, Erk activation, via integrins α6 and β4, may be correlated with the proliferation, rather than with invasion, of GBM cells. The results of these previous studies are in agreement with our results, indicating that U87-Inv cells showed a decrease in cell proliferation with the downregulation of integrin α6β4 and Erk. Interestingly, we found that highly invasive GBM cells showed decreased proliferation. Several previous studies confirm that the levels of invasiveness are inversely related to the rate of proliferation (32, 61). These studies also indicate that the invasiveness of GBM was correlated with stem-like characteristics and suggest that tumor cells with stem-like characteristics have a lower rate of proliferation (32). The invasiveness and proliferation of GBM may be controlled by different and exclusive mechanisms. Previous studies report that Akt is activated by the RTK/PTEN/PI3K pathway, which helps glioma cells grow uncontrollably and become invasive (32, 62); however, we could not find the same correlation (Figure 5B).

Since the GBM comprises a heterogeneous mixture of functionally distinct cancer cells, there is a difference in molecular expression, invasiveness, proliferation and morphology between each GBM cell line (63, 64). Thus, we attempted to analyze comparatively between U87MG and U373MG cells. The U373MG cells showed increased proliferative activity and integrin β4 expression whereas decreased invasiveness compared with that of U87MG cells. However, there was no significant difference in integrin a6 expression between U373MG and U87MG cells. For deeper insight into integrin β4 expression, transfection and knockout experiments were performed in each cell lines. Our results showed that expression of integrin β4 was positively correlated with proliferation and negatively with invasiveness, which was consistent with the above experiments of U87-Inv and U87-Non cells.

Integrin β4 has been studied more actively in other cancers than GBM. Unlike our results, integrin β4 expression is correlated to invasiveness in other cancers including breast cancer, hepatocellular carcinoma, pancreatic cancer and squamous cell carcinoma of skin (65-68). We tried to clinicopathologically evaluate integrin β4 expression in human GBM tissue for solid result. The proliferation potential of GBM cells was measured by Ki-67 immuno-staining, which demonstrated that GBM cells proliferation was significantly correlated with integrin β4 expression (Table 2 and Figure 10). Radiological evaluation for multiplicity of GBM can be a clinical method of assessing invasiveness. Our results showed that integrin β4 expression was negatively correlated with the multiplicity and relapse of the GBM (Table 3). We might prove that integrin β4 expression was positively correlated with proliferation and negatively with invasiveness in GBM patients, which was

consistent with the cell line experiments.

In conclusion, using a laminin-2 substrate, we selected a highly invasive subpopulation of cells from the U78MG cell line and showed that U87-Inv cells possess highly invasive characteristics. Moreover, we attempted a comparative analysis to identify differences between U87MG and U373MG cells. We found that activation of the integrin β4 enhanced the proliferation, whereas decreased invasiveness in GBM cell line. Notably, the consistent result was observed in TMA study. To our knowledge, this is the first study to evaluate clinicopathological feature and prognostic value of integrin β4 expression in GBM patients.

REFERENCES

1. Stupp R, Mason WP, van den Bent MJ, Weller M, Fisher B, Taphoorn MJ, et al. Radiotherapy plus concomitant and adjuvant temozolomide for glioblastoma. N Engl J Med. 2005;352(10):987-96.

2. Giese A, Westphal M. Glioma invasion in the central nervous system. Neurosurgery. 1996;39(2):235-50; discussion 50-2.

3. Chintala SK, Rao JK. Invasion of human glioma: role of extracellular matrix proteins. Frontiers in bioscience : a journal and virtual library. 1996;1:d324-39.

4. Tisi D, Talts JF, Timpl R, Hohenester E. Structure of the C-terminal laminin G-like domain pair of the laminin alpha2 chain harbouring binding sites for alpha-dystroglycan and heparin. EMBO J. 2000;19(7):1432-40.

5. Leivo I, Engvall E. Merosin, a protein specific for basement membranes of Schwann cells, striated muscle, and trophoblast, is expressed late in nerve and muscle development. Proceedings of the National Academy of Sciences of the United States of America. 1988;85(5):1544-8.

6. Patarroyo M, Tryggvason K, Virtanen I. Laminin isoforms in tumor invasion, angiogenesis and metastasis. Seminars in cancer biology. 2002;12(3):197-207.

7. Jones KJ, Morgan G, Johnston H, Tobias V, Ouvrier RA, Wilkinson I, et al. The expanding phenotype of laminin alpha2 chain (merosin) abnormalities: case series and review. J Med Genet. 2001;38(10):649-57.

8. Helbling-Leclerc A, Zhang X, Topaloglu H, Cruaud C, Tesson F,

Weissenbach J, et al. Mutations in the laminin alpha 2-chain gene (LAMA2) cause merosin-deficient congenital muscular dystrophy. Nature genetics. 1995;11(2):216-8.

9. Masaki T, Matsumura K, Saito F, Yamada H, Higuchi S, Kamakura K, et al. Association of dystroglycan and laminin-2 coexpression with myelinogenesis in peripheral nerves. Medical electron microscopy : official journal of the Clinical Electron Microscopy Society of Japan. 2003;36(4):221-39.

10. Giese A, Kluwe L, Laube B, Meissner H, Berens ME, Westphal M. Migration of human glioma cells on myelin. Neurosurgery. 1996;38(4):755-64.

11. Inda MM, Bonavia R, Mukasa A, Narita Y, Sah DW, Vandenberg S, et al. Tumor heterogeneity is an active process maintained by a mutant EGFR-induced cytokine circuit in glioblastoma. Genes Dev. 2010;24(16):1731-45.

12. Harada K, Nishizaki T, Ozaki S, Kubota H, Ito H, Sasaki K. Intratumoral cytogenetic heterogeneity detected by comparative genomic hybridization and laser scanning cytometry in human gliomas. Cancer Res. 1998;58(20):4694-700.

13. Shapiro JR, Yung WK, Shapiro WR. Isolation, karyotype, and clonal growth of heterogeneous subpopulations of human malignant gliomas. Cancer Res. 1981;41(6):2349-59.

14. Wikstrand CJ, Bigner SH, Bigner DD. Demonstration of complex antigenic heterogeneity in a human glioma cell line and eight derived clones by specific monoclonal antibodies. Cancer Res. 1983;43(7):3327-34.

15. Lu KV, Jong KA, Rajasekaran AK, Cloughesy TF, Mischel PS. Upregulation of tissue inhibitor of metalloproteinases (TIMP)-2 promotes matrix metalloproteinase (MMP)-2 activation and cell invasion in a human glioblastoma

cell line. Laboratory investigation; a journal of technical methods and pathology. 2004;84(1):8-20.

16. Fujiwara H, Kikkawa Y, Sanzen N, Sekiguchi K. Purification and characterization of human laminin-8. Laminin-8 stimulates cell adhesion and migration through alpha3beta1 and alpha6beta1 integrins. J Biol Chem. 2001;276(20):17550-8.

17. Delwel GO, de Melker AA, Hogervorst F, Jaspars LH, Fles DL, Kuikman I, et al. Distinct and overlapping ligand specificities of the alpha 3A beta 1 and alpha 6A beta 1 integrins: recognition of laminin isoforms. Mol Biol Cell. 1994;5(2):203-15.

18. Yao CC, Ziober BL, Squillace RM, Kramer RH. Alpha7 integrin mediates cell adhesion and migration on specific laminin isoforms. J Biol Chem. 1996;271(41):25598-603.

19. Hynes RO. Integrins: bidirectional, allosteric signaling machines. Cell. 2002;110(6):673-87.

20. Gilbertson RJ, Rich JN. Making a tumour's bed: glioblastoma stem cells and the vascular niche. Nat Rev Cancer. 2007;7(10):733-6.

21. Hood JD, Cheresh DA. Role of integrins in cell invasion and migration. Nat Rev Cancer. 2002;2(2):91-100.

22. Gladson CL. Expression of integrin alpha v beta 3 in small blood vessels of glioblastoma tumors. J Neuropathol Exp Neurol. 1996;55(11):1143-9.

23. Tabatabai G, Weller M, Nabors B, Picard M, Reardon D, Mikkelsen T, et al. Targeting integrins in malignant glioma. Target Oncol. 2010;5(3):175-81.

24. Scaringi C, Minniti G, Caporello P, Enrici RM. Integrin inhibitor

cilengitide for the treatment of glioblastoma: a brief overview of current clinical results. Anticancer Res. 2012;32(10):4213-23.

25. Nakada M, Nambu E, Furuyama N, Yoshida Y, Takino T, Hayashi Y, et al. Integrin alpha3 is overexpressed in glioma stem-like cells and promotes invasion. Br J Cancer. 2013;108(12):2516-24.

26. Lathia JD, Gallagher J, Heddleston JM, Wang J, Eyler CE, Macswords J, et al. Integrin alpha 6 regulates glioblastoma stem cells. Cell Stem Cell. 2010;6(5):421-32.

27. Hu Y, Ylivinkka I, Chen P, Li L, Hautaniemi S, Nyman TA, et al. Netrin-4 promotes glioblastoma cell proliferation through integrin beta4 signaling. Neoplasia. 2012;14(3):219-27.

28. Kwiatkowska A, Symons M. Signaling determinants of glioma cell invasion. Advances in experimental medicine and biology. 2013;986:121-41.

29. Thomas SL, Alam R, Lemke N, Schultz LR, Gutierrez JA, Rempel SA. PTEN augments SPARC suppression of proliferation and inhibits SPARC-induced migration by suppressing SHC-RAF-ERK and AKT signaling. Neuro Oncol. 2010;12(9):941-55.

30. Velpula KK, Rehman AA, Chelluboina B, Dasari VR, Gondi CS, Rao JS, et al. Glioma stem cell invasion through regulation of the interconnected ERK, integrin alpha6 and N-cadherin signaling pathway. Cell Signal. 2012;24(11):2076-84.

31. Chen D, Zuo D, Luan C, Liu M, Na M, Ran L, et al. Glioma cell proliferation controlled by ERK activity-dependent surface expression of PDGFRA. PLoS One. 2014;9(1):e87281.

32. Molina JR, Hayashi Y, Stephens C, Georgescu MM. Invasive glioblastoma cells acquire stemness and increased Akt activation. Neoplasia. 2010;12(6):453-63.

33. Hashimoto Y, Kim DJ, Adams JC. The roles of fascins in health and disease. J Pathol. 2011;224(3):289-300.

34. Hashimoto Y, Skacel M, Adams JC. Roles of fascin in human carcinoma motility and signaling: prospects for a novel biomarker? Int J Biochem Cell Biol. 2005;37(9):1787-804.

35. Hashimoto Y, Parsons M, Adams JC. Dual actin-bundling and protein kinase C-binding activities of fascin regulate carcinoma cell migration downstream of Rac and contribute to metastasis. Mol Biol Cell. 2007;18(11):4591-602.

36. Hwang JH, Smith CA, Salhia B, Rutka JT. The role of fascin in the migration and invasiveness of malignant glioma cells. Neoplasia. 2008;10(2):149-59.

37. Jayo A, Parsons M. Fascin: a key regulator of cytoskeletal dynamics. Int J Biochem Cell Biol. 2010;42(10):1614-7.

38. Dingemans AM, van den Boogaart V, Vosse BA, van Suylen RJ, Griffioen AW, Thijssen VL. Integrin expression profiling identifies integrin alpha5 and beta1 as prognostic factors in early stage non-small cell lung cancer. Molecular cancer. 2010;9:152.

39. Schmittgen TD, Livak KJ. Analyzing real-time PCR data by the comparative C(T) method. Nature protocols. 2008;3(6):1101-8.

40. Louis DN, Perry A, Reifenberger G, von Deimling A, Figarella-Branger D, Cavenee WK, et al. The 2016 World Health Organization Classification of Tumors

of the Central Nervous System: a summary. Acta neuropathologica. 2016;131(6):803-20.

41. Esteller M, Garcia-Foncillas J, Andion E, Goodman SN, Hidalgo OF, Vanaclocha V, et al. Inactivation of the DNA-repair gene MGMT and the clinical response of gliomas to alkylating agents. N Engl J Med. 2000;343(19):1350-4.

42. Ambros PF, Ambros IM. Pathology and biology guidelines for resectable and unresectable neuroblastic tumors and bone marrow examination guidelines. Medical and pediatric oncology. 2001;37(6):492-504.

43. Wang M, Wang T, Liu S, Yoshida D, Teramoto A. The expression of matrix metalloproteinase-2 and -9 in human gliomas of different pathological grades. Brain Tumor Pathol. 2003;20(2):65-72.

44. Du R, Petritsch C, Lu K, Liu P, Haller A, Ganss R, et al. Matrix metalloproteinase-2 regulates vascular patterning and growth affecting tumor cell survival and invasion in GBM. Neuro Oncol. 2008;10(3):254-64.

45. Takano S, Tian W, Matsuda M, Yamamoto T, Ishikawa E, Kaneko MK, et al. Detection of IDH1 mutation in human gliomas: comparison of immunohistochemistry and sequencing. Brain Tumor Pathol. 2011;28(2):115-23.

46. Yan H, Parsons DW, Jin G, McLendon R, Rasheed BA, Yuan W, et al. IDH1 and IDH2 mutations in gliomas. N Engl J Med. 2009;360(8):765-73.

47. Rivera AL, Pelloski CE, Gilbert MR, Colman H, De La Cruz C, Sulman EP, et al. MGMT promoter methylation is predictive of response to radiotherapy and prognostic in the absence of adjuvant alkylating chemotherapy for glioblastoma. Neuro Oncol. 2010;12(2):116-21.

48. Tardy M. Role of laminin bioavailability in the astroglial permissivity for

neuritic outgrowth. An Acad Bras Cienc. 2002;74(4):683-90.

49. Costa S, Planchenault T, Charriere-Bertrand C, Mouchel Y, Fages C, Juliano S, et al. Astroglial permissivity for neuritic outgrowth in neuron-astrocyte cocultures depends on regulation of laminin bioavailability. Glia. 2002;37(2):105-13.

50. Aplin AE, Juliano RL. Integrin and cytoskeletal regulation of growth factor signaling to the MAP kinase pathway. J Cell Sci. 1999;112 (Pt 5):695-706.

51. Boudjadi S, Carrier JC, Beaulieu JF. Integrin alpha1 subunit is up-regulated in colorectal cancer. Biomark Res. 2013;1(1):16.

52. Macias-Perez I, Borza C, Chen X, Yan X, Ibanez R, Mernaugh G, et al. Loss of integrin alpha1beta1 ameliorates Kras-induced lung cancer. Cancer Res. 2008;68(15):6127-35.

53. Heller KN, Montgomery CL, Shontz KM, Clark KR, Mendell JR, Rodino-Klapac LR. Human alpha7 Integrin Gene (ITGA7) Delivered by Adeno-Associated Virus Extends Survival of Severely Affected Dystrophin/Utrophin-Deficient Mice. Hum Gene Ther. 2015.

54. Ren B, Yu YP, Tseng GC, Wu C, Chen K, Rao UN, et al. Analysis of integrin alpha7 mutations in prostate cancer, liver cancer, glioblastoma multiforme, and leiomyosarcoma. J Natl Cancer Inst. 2007;99(11):868-80.

55. Lipscomb EA, Simpson KJ, Lyle SR, Ring JE, Dugan AS, Mercurio AM. The alpha6beta4 integrin maintains the survival of human breast carcinoma cells in vivo. Cancer Res. 2005;65(23):10970-6.

56. Lu S, Simin K, Khan A, Mercurio AM. Analysis of integrin beta4 expression in human breast cancer: association with basal-like tumors and

prognostic significance. Clin Cancer Res. 2008;14(4):1050-8.

57. Chung J, Bachelder RE, Lipscomb EA, Shaw LM, Mercurio AM. Integrin (alpha 6 beta 4) regulation of eIF-4E activity and VEGF translation: a survival mechanism for carcinoma cells. J Cell Biol. 2002;158(1):165-74.

58. Nikolopoulos SN, Blaikie P, Yoshioka T, Guo W, Giancotti FG. Integrin beta4 signaling promotes tumor angiogenesis. Cancer Cell. 2004;6(5):471-83.

59. Delamarre E, Taboubi S, Mathieu S, Berenguer C, Rigot V, Lissitzky JC, et al. Expression of integrin alpha6beta1 enhances tumorigenesis in glioma cells. The American journal of pathology. 2009;175(2):844-55.

60. Corsini NS, Martin-Villalba A. Integrin alpha 6: anchors away for glioma stem cells. Cell Stem Cell. 2010;6(5):403-4.

61. Mariani L, Beaudry C, McDonough WS, Hoelzinger DB, Demuth T, Ross KR, et al. Glioma cell motility is associated with reduced transcription of proapoptotic and proliferation genes: a cDNA microarray analysis. J Neurooncol. 2001;53(2):161-76.

62. McDowell KA, Riggins GJ, Gallia GL. Targeting the AKT pathway in glioblastoma. Current pharmaceutical design. 2011;17(23):2411-20.

63. Motaln H, Koren A, Gruden K, Ramsak Z, Schichor C, Lah TT. Heterogeneous glioblastoma cell cross-talk promotes phenotype alterations and enhanced drug resistance. Oncotarget. 2015;6(38):40998-1017.

64. Koo S, Martin GS, Schulz KJ, Ronck M, Toussaint LG. Serial selection for invasiveness increases expression of miR-143/miR-145 in glioblastoma cell lines. BMC cancer. 2012;12:143.

65. Li XL, Liu L, Li DD, He YP, Guo LH, Sun LP, et al. Integrin beta4

promotes cell invasion and epithelial-mesenchymal transition through the modulation of Slug expression in hepatocellular carcinoma. Scientific reports. 2017;7:40464.

66. Masugi Y, Yamazaki K, Emoto K, Effendi K, Tsujikawa H, Kitago M, et al. Upregulation of integrin beta4 promotes epithelial-mesenchymal transition and is a novel prognostic marker in pancreatic ductal adenocarcinoma. Laboratory investigation; a journal of technical methods and pathology. 2015;95(3):308-19.

67. Moilanen JM, Loffek S, Kokkonen N, Salo S, Vayrynen JP, Hurskainen T, et al. Significant Role of Collagen XVII And Integrin beta4 in Migration and Invasion of The Less Aggressive Squamous Cell Carcinoma Cells. Scientific reports. 2017;7:45057.

68. Gerson KD, Shearstone JR, Maddula VS, Seligmann BE, Mercurio AM. Integrin beta4 regulates SPARC protein to promote invasion. J Biol Chem. 2012;287(13):9835-44.

국문 초록

이 규 상

의학과 중개의학전공

서울대학교 의과대학

서론: 교모세포종은 악성 신경교종으로 침습능이 매우 강력하여 종양의 완전한 수술적 절제는 거의 불가능하다. 따라서 우리 연구에서는 교모세포종의 이런 침습능을 연구하기 위하여 메로신에서 U87MG 세포주를 배양하여 침습성이 더욱 강한 세포를 분리하였고 U87MG와 U373MG 두 세포주 간의 특징을 비교 분석하였다. 더 나아가 우리는 교모세포종에서 integrin β4 발현의 의미, 임상 병리학적 특징과 예후에 대해 중점적으로 연구 하였다.

방법: 우리는 laminin-2가 코팅된 transwell 필터를 사용하여 U87MG 세포주에서 침습능이 강한 10 %의 세포 (U87-Inv)를 선정하였다. 그리고 matrix metalloproteinase-2 (MMP-2), fascin, integrin의 subunit들, Akt 및 Erk를 포함한 침습능 관련 인자들의 발현을 평가했으며 상처 치유 실험을 시도하였다. 그리고 젤라틴 zymography, 세포 증식 분석, integrin의 subunit들 발현 분석을 위한 실시간 정량적 중합 효소 연쇄 반응 (RT-qPCR), fascin, Akt 및 Erk

발현 분석을 위한 western blot 및 fascin과 actin에 대한 immunofluorescence를 시행하였다. Integrin β4의 기능을 중점적으로 평가하기 위해 U87MG 세포주에서는 pRK5 β4 플라스미드 DNA를 이용한 transfection을 시도 하였고 U373MG 세포주에서는 integrin β4 shRNA 이용한 knockout 방법을 사용하였다. 더욱이 89 명의 교모세포종 환자의 후향적 코호트에서 integrin β4 발현을 면역조직화학 검사를 통해 분석하였으며 세포질에 중등도 또는 강한 강도로 염색이 되었을 때 양성으로 간주하였다. 추가적으로 EGFR, p53, IDH-1 및 Ki-67을 면역조직화학 검사를 통해 분석하였다.

결과: U87-Inv 세포의 이동 속도는 비교적 덜 침습적 인 세포(U87-Non)에 비해 약 20 % 증가하였고 빠른 상처 치유 능력을 보였지만 증식 능력은 높지 않았다. U87- Inv 세포에서는 광범위한 lamellipodia의 확장, fascin, actin, MMP-2의 발현 증가가 관찰되었지만 ERK의 발현은 감소되었다. 또한 U87-Inv에서 integrin α6과 β4가 약 0.4 및 0.6 배 감소된 반면 integrin α1와 α7의 발현은 약 1.5 배 증가 하였다. U373MG 세포와 U87MG 비교 실험에서 U373MG 세포가 U87MG 세포보다 이동 속도는 느리고 증식 능력은 더 높았는데 흥미롭게도 U373MG는 U87MG 세포에 비해 integrin β4 발현이 현저하게 증가되었다. pRK5 β4로 integrin β4가 삽입된 U87MG 세포는 대조군 U87MG 세포보다 이동 속도는 느려지고 증식 능력은

증가되었다. Integrin β4가 knockout된 U373MG 세포는 대조군 U373MG 세포보다 빠른 이동 속도와 감소된 증식 능력을 보였다. 이런 우리 실험의 결과는 integrin β4의 발현이 교모세포종 세포주에서 증식과는 양의 상관관계, 침습능과는 음의 상관관계 있음을 설명한다. 교모세포종 환자에서 integrin β4의 발현을 분석해보면 전체 중 33 명 (37.1 %)의 환자에서 관찰되었다. Ki-67 발현과 통계적으로 유의한 상관관계가 있었고 교모세포종의 다발성 및 재발과 관련이 있었다. 따라서 integrin β4의 발현은 교모세포종 환자에서 종양 증식에 중요한 역할을 하지만 침습능과는 음의 상관 관계가 있는 것으로 생각된다. Kaplan-Meier 분석 결과에서는 integrin β4의 발현은 교모세포종 환자의 예후와는 상관성이 없었다.

결론: 본 연구에서는 laminin-2을 세포 배양 기질로 사용하여 침습성이 강한 교모세포종 세포주의 소집단을 성공적으로 분리하였다. 이 세포주는 integrin α6와 β4 및 Erk 발현 감소되었고 증식 능력도 동반 감소를 보였다. 또한, 교모세포종에서 integrin β4의 역할에 대한 평가에 초점을 두었고 integrin β4가 발현된 교모세포종 환자에서 임상 병리학적 특징 및 예후에 대한 분석을 시행하였다. 결론적으로, 우리의 연구 결과는 integrin β4의 발현이 교모세포종의 침습능과는 음의 상관관계에 있으며, 이와는 반대로 증식 능력과는 양의 상관 관계가 있음을 보여주었다.

주요어 : 교모세포종, 인테그린 $\beta 4$, 침습능, 증식능, 메로신

학 번 : 2012-30558